Chapter 9
Nuclear Reactions

Michael Wiescher[1] **and Thomas Rauscher**[2]

Nuclear reaction rates determine the abundances of isotopes in stellar burning processes. A multitude of reactions determine the reaction flow pattern which is described in terms of reaction network simulations. The reaction rates are determined by laboratory experiments supplemented by nuclear reaction and structure theory. We will discuss the experimental approach as well as the theoretical tools for obtaining the stellar reaction rates. A detailed analysis of a reaction is only possible for a few selected cases which will be highlighted in this section. The bulk of nuclear reaction processes is however described in terms of a statistical model approach, which relies on global nuclear structure and reaction parameters such as level density and mass and barrier penetration, respectively. We will discuss a variety of experimental facilities and techniques used in the field, this includes low energy stable beam experiments, measurements at radioactive beam accelerators, and neutron beam facilities.

9.1 Nuclear Reactions in Astrophysical Environments

Nuclear reactions are the engine of stellar evolution and determine the overall production of the long-lived radioactive isotopes in a variety of nucleosynthesis patterns. A detailed understanding of the characteristic production and depletion rates within the framework of the nucleosynthesis process is crucial for reliable model predictions and the interpretation of the observed abundances.

There are several experimental and theoretical challenges in obtaining stellar reaction rates. The interaction energies in stellar environments extend from basically zero projectile energy up to only several MeV. This is especially challenging for the measurement of the relevant reaction cross sections which can be extremely small, especially for reactions with charged projectiles. This also makes theoretical pre-

[1] University of Notre Dame, Notre Dame, IN 46556, USA
[2] Universität Basel, 4056 Basel, Switzerland

dictions extremely difficult because several reaction mechanisms (see below) may compete and simpler approximations may only be of limited use.

Another challenge arises from the fact that nuclear burning at high temperature produces very short-lived isotopes which subsequently decay to long-lived and stable species. Current experimental technology can only access a fraction of those yet and is still limited in obtaining detailed information on their properties. The possibility to measure cross sections of reactions with such highly unstable nuclei is even more limited currently. Thus, investigations of nucleosynthesis in high-temperature environments largely rely on theoretical models, which not only have to treat the reaction mechanisms properly but also are required to predict nuclear properties far from stability.

Moreover, depending on the actual plasma conditions, reactions in an astrophysical plasma may proceed fundamentally differently from those in the laboratory. This is due to two effects. On one hand, laboratory nuclei are always part of atoms or molecules whereas astrophysical nuclear burning involves fully ionized nuclei immersed in a cloud of free electrons (and photons). The Coulomb charge of a nucleus is partially shielded by the surrounding electrons but this shielding (or screening) effect will be different for an atom or molecule and a plasma because of the different electron distribution and kinetics. While theoretical cross sections always imply bare nuclei, the values have to be appropriately converted (also based on a theoretical treatment of different screening mechanisms) for comparison to low-energy laboratory cross sections and for application in astrophysical plasmas. Additionally, the quantum mechanically and geometrically different electron distribution in a plasma directly affects electron capture reactions. For example, nuclei such as ^{7}Be or ^{44}Ti, decaying by capturing an electron from the K-shell of the atom under laboratory conditions will not be able to do this in a stellar plasma. Instead, electron capture inside a star involves capturing a free electron from the plasma, which is more unlikely and therefore the terrestrial half-life can be shorter than the one in a stellar environment (Iliadis, 2007; Johnson et al., 1992).

Finally, due to the high photon and matter densities in astrophysical environments, nuclei very quickly reach thermal equilibrium with the surroundings by excitation and de-excitation via photons and by collisions. In most cases, this happens on a shorter timescale than that of nuclear transformations (one of the exceptions being isomeric states). Consequently, the nuclei involved in the reactions occur not only in their ground states, as in the laboratory, but also their excited states are populated with a probability involving the Boltzmann factor. So far, reactions on excited states can only be treated theoretically. The population of excited nuclear states does not only depend on the plasma temperature but also on the structure of a nucleus. Nuclei with isolated levels reachable within a few keV projectile energy will exhibit pronounced thermal population already at low plasma temperature. This is especially important for modern s-process studies which require high accuracy knowledge of neutron capture rates. Thermal effects are also important in decays and neutrino reactions because the available phase space of the reaction products is altered, leading to a modification of the rate. For example, electron capture rates in the stellar core

collapse are enhanced at temperatures $T > 1.5$ MeV because of the unblocking of low-lying neutron states by thermal excitation (Cooperstein et al., 1984).

9.1.1 Reaction Networks and Thermonuclear Reaction Rates

The change of abundances Y with time due to nuclear processes is traced by coupled differential equations. To be fully solvable, the number of equations N must equal the number of involved nuclei acting as reaction partners and thus an equation matrix of size N^2 has to be solved. Such a set of coupled equations is called reaction network and can generally be written as

$$\dot{Y}_i = \frac{1}{\rho N_\mathrm{A}} \dot{n}_i = \frac{1}{\rho N_\mathrm{A}} \left\{ \sum_j {}^1_i P_j \, {}_i\lambda_j + \sum_j {}^2_i P_j \, {}_i r_j + \sum_j {}^3_i P_j \, {}_i\hat{r}_j + \ldots \right\} \quad , \tag{9.1}$$

where $1 \leq i \leq N$ numbers the nucleus, ${}_i\lambda_j$ is the jth rate for destruction or creation of the ith nucleus without a nuclear projectile involved (this includes spontaneous decay, lepton capture, photodisintegration), and ${}_i r_j$ is the rate of the jth reaction involving a nuclear projectile and creating or destroying nucleus i. Similarly, we have three-body reactions where nucleus i is produced or destroyed together with two other (or similar) nuclei. Reactions with more participants (denoted by $\ldots$ above) are unlikely to occur at astrophysical conditions and are usually neglected. The quantities ${}^1_i P_j$, ${}^2_i P_j$, and ${}^3_i P_{jk}$ are positive or negative integer numbers specifying the amount of nuclei i produced or destroyed, respectively, in the given process. As shown below, the rates λ, r, and $\hat{r}$ contain the abundances of the interacting nuclei. Rates of type λ depend on one abundance (or number density), rates r depend on the abundances of two species, and rates $\hat{r}$ on three.

Using abundances Y instead of number densities $n = Y\rho N_\mathrm{A}$ (where ρ is the plasma density) has the advantage that a change in the number of nuclei in a given volume due to density fluctuations is factored out and only changes by nuclear processes are considered. Using abundance changes, the total energy generation rate per mass due to nuclear reactions can easily be expressed as

$$\dot{\varepsilon} = -\sum_i \dot{Y}_i N_A M_i c^2 \quad , \tag{9.2}$$

with the rest masses $M_i c^2$ of the participating nuclei.

The rates ${}_i\lambda_j$ appearing in the first term of Eq. 9.1 are reactions per time and volume, and only contain the abundance Y_j. For example, ${}_i\lambda_j$ is simply $n_j L_j = Y_j \rho N_\mathrm{A} L_j$ for β-decays. The factor $L_j = (\ln 2)/{}^j T_{1/2}$ is the usual decay constant (with the unit 1/time) and is related to the half-life ${}^j T_{1/2}$ of the decaying nucleus j. It has to be noted that some decays depend on the plasma temperature and thus L_j is not always constant, even for decays.

Two-body rates r include the abundances of two interacting particles or nuclei. In general, target and projectile follow specific thermal momentum distributions dn_1 and dn_2 in an astrophysical plasma. With the resulting relative velocities $\mathbf{v}_1 - \mathbf{v}_2$, the number of reactions per volume and time, is given by

$$r_{12} = \int \hat{\sigma}(|\mathbf{v}_1 - \mathbf{v}_2|)|\mathbf{v}_1 - \mathbf{v}_2| dn_1 dn_2 \quad , \tag{9.3}$$

and involves the reaction cross section $\hat{\sigma}$ as a function of velocity/energy, the relative velocity $\mathbf{v}_1 - \mathbf{v}_2$ and the thermodynamic distributions of target and projectile dn_1 and dn_2. The evaluation of this integral depends on the type of particles (fermions, bosons) and distributions which are involved.

However, many two-body reactions can be simplified and effectively expressed similarly to one-body reactions, only depending on one abundance (or number density). If reaction partner 2 is a photon, the relative velocity is always c and the quantities in the integral do not depend on dn_1. This simplifies the rate expression to

$$\lambda_1 = L_\gamma(T) n_1 \quad , \tag{9.4}$$

where $L_\gamma(T)$ stems from an integration over a Planck distribution for photons of temperature T. This is similar to the decay rates introduced earlier and therefore we replaced r by λ in our notation and can include this type of reaction in the first term of Eq. 9.1. A similar procedure is used for electron captures by protons and nuclei. Because the electron is about 2000 times less massive than a nucleon, the velocity of the nucleus is negligible in the center-of-mass system in comparison to the electron velocity ($|\mathbf{v}_{\rm nucleus} - \mathbf{v}_{\rm electron}| \approx |\mathbf{v}_{\rm electron}|$). The electron capture cross section has to be integrated over a Fermi distribution of electrons. The electron capture rates are a function of T and $n_e = Y_e \rho N_A$, the electron number density. In a neutral, completely ionized plasma, the electron abundance Y_e is equal to the total proton abundance $Y_e = \sum_i Z_i Y_i$ and thus

$$\lambda_{\rm nucleus,ec} = L_{\rm ec}(T, \rho Y_e) n_{\rm nucleus} \quad . \tag{9.5}$$

Again, we have effectively a rate per target L (with unit 1/time) similar to the treatment of decays earlier and a rate per volume including the number density of only one nucleus. We denote the latter by λ and use it in the first term of Eq. 9.1. This treatment can be applied also to the capture of positrons, being in thermal equilibrium with photons, electrons, and nuclei. Furthermore, at high densities ($\rho > 10^{12} {\rm gcm}^{-3}$) the size of the neutrino scattering cross section on nucleons, nuclei, and electrons ensures that enough scattering events occur to lead to a continuous neutrino energy distribution. Then also the inverse process to electron capture (neutrino capture) can occur as well as other processes like, e.g., inelastic scattering, leaving a nucleus in an excited state which can emit nucleons and α particles. Such reactions can be expressed similarly to photon and electron captures, integrating over the corresponding neutrino distribution.

In the following, we focus on the case of two interacting nuclei or nucleons as these reactions will be extensively discussed in Secs. 9.3 and 9.4. This will result in

an actual two-body rate r to be used in the second term of Eq. 9.1. Here, we mention in passing that Eq. 9.3 can be generalized to 3 and more interacting nuclear species by integrating over the appropriate number of distributions, leading to rates $\hat{r}$ and higher order terms in Eq. 9.1.

Turning our attention back to two-body reactions, we note that the velocity distributions can be replaced by energy distributions. Furthermore, it can be shown that the two distributions in Eq. 9.3 can be replaced by a single one in the center-of-mass system. This time the resulting expression describes a rate r including two abundances (or number densities) and showing up in the second term of Eq. 9.1. The rate r is defined as an interaction of two reaction partners with an energy distribution $\phi(E)$ according to the plasma temperature T and a reaction cross section $\sigma(E)$ specifying the probability of the reaction in the plasma:

$$r = \frac{n_1 n_2}{1+\delta_{12}} \int_0^\infty \sigma(E)\phi(E)\,dE \quad . \tag{9.6}$$

The factor $1/(1+\delta_{12})$ with the Kronecker symbol δ is introduced to avoid double counting. The nuclear cross section is defined as in standard scattering theory by

$$\sigma = \frac{\text{number of reactions target}^{-1}\text{sec}^{-1}}{\text{flux of incoming projectiles}} \quad . \tag{9.7}$$

However, in an astrophysical plasma, nuclei quickly (on the timescale of nuclear reactions and scattering) reach thermal equilibrium with all plasma components. This allows thermal excitation of nuclei which follows a Boltzmann law and gives rise to the *stellar* reaction rate

$$\begin{aligned} r^* &= \frac{n_1 n_2}{1+\delta_{12}} \frac{1}{\sum_x (2J_x+1)e^{-\frac{E_x}{kT}}} \sum_x \left\{ (2J_x+1) \int_0^\infty \sigma^x(E^x)\phi(E^x)e^{-\frac{E_x}{kT}}\,dE^x \right\} \\ &= \frac{n_1 n_2}{1+\delta_{12}} \frac{1}{G(T)} \sum_x \left\{ (2J_x+1) \int_0^\infty \sigma^x(E^x)\phi(E^x)e^{-\frac{E_x}{kT}}\,dE^x \right\} \quad , \end{aligned} \tag{9.8}$$

where the sum runs over all excited states x of the target (for simplicity, here we assume the projectile, i.e. the second reaction partner, does not have excited states) with spin J_x and excitation energy E_x. The quantity G is the partition function of the nucleus. The cross section σ^x includes the reactions commencing from excited state x and they are functions of the energy E^x relative to this excited state. Cross sections $\sigma = \sigma^{x=0}$ measured in terrestrial laboratories do not include such thermal effects. At low temperature (e.g., for the s-process) the stellar enhancement factor $\text{SEF} = r^*/r$ will only differ from unity when there are excited states within a few keV above the reaction threshold. At the large temperatures reached in explosive burning, thermal enhancement can lead to a considerable deviation from the ground-state cross section, see also Rauscher (2011).

Nuclei in an astrophysical plasma obey a Maxwell-Boltzmann (MB) distribution $\phi(E) = \phi_{\text{MB}}$ and we obtain finally (Rauscher, 2011):

$$r = \frac{n_1 n_2}{1+\delta_{12}} < \sigma v >^* \quad , \tag{9.9}$$

$$< \sigma v >^* = (\frac{8}{\mu \pi})^{1/2} (kT)^{-3/2} \frac{1}{G(T)} \sum_x \left\{ (2J_x+1) \int_0^\infty E^x \sigma^x(E^x) e^{-\frac{E^x+E_x}{kT}} \, dE^x \right\} \quad . \tag{9.10}$$

Here, μ denotes the reduced mass of the two-particle system and $< \sigma v >^*$ is the stellar reaction rate per particle pair or *reactivity*.

As mentioned above the charge of the reaction partners can be screened. For most astrophysical conditions this can be included by introducing a screening factor $f_{\rm screen}$, modifying the above rate for bare nuclei (Iliadis, 2007; Salpeter et al., 1969)

$$r^{\rm scr} = f_{\rm screen} r \quad . \tag{9.11}$$

The screening factor is derived from the plasma conditions of the specific stellar environment. At high densities and low temperatures screening factors can enhance reactions by many orders of magnitude and lead to *pycnonuclear ignition* (Yakovlev et al., 2006). However, note that the above factorization is not valid for vanishing temperatures when nuclei are trapped in a Coulomb lattice.

Forward and reverse rates are related. Applying the well-known reciprocity theorem for nuclear transitions (Blatt, et al., 1991) and further assuming that the reactands in the entrance channel a as well as the reaction products in the exit channel b are instantaneously thermalized (the *detailed balance* principle), the relation (Holmes et al., 1976; Iliadis, 2007)

$$< \sigma v >^*_{b \to a} = \frac{1+\delta_{b_1 b_2}}{1+\delta_{a_1 a_2}} \frac{G_{a_1} G_{a_2}}{G_{b_1} G_{b_2}} \left(\frac{\mu_a}{\mu_b} \right)^{3/2} e^{-\frac{Q}{kT}} < \sigma v >^*_{a \to b} \quad , \tag{9.12}$$

relating the *stellar* reverse rate to the *stellar* forward rate. The latter has the reaction Q-value Q. For captures (forward channel a) and photodisintegrations (reverse channel b), Eq. 9.12 transforms to

$$L_\gamma = \frac{1}{1+\delta_{a_1 a_2}} \frac{G_{a_1} G_{a_2}}{G_b} \left(\frac{\mu_a kT}{2\pi\hbar^2} \right)^{3/2} e^{-\frac{Q}{kT}} < \sigma v >^*_{\rm capture} \quad . \tag{9.13}$$

These expressions will not be valid anymore if any of the involved rates was derived from a laboratory cross section. They also imply that the detailed balance assumption is valid. Detailed balance can be violated in nuclei with long-lived isomeric states which are not populated or depopulated during regular reaction timescales. For these cases, reactions to separate final states have to be calculated and the (de)population of these states by photon transitions followed explicitly (Ward et al., 1980). Important examples for such nuclei are ^{26}Al and ^{180}Ta (Rauscher et al., 2002).

9.1.2 Reaction Equilibria

It is not always necessary to solve a full reaction network (Eq. 9.1) including all the rates. On one hand, simplifications can often be made by omitting slow reactions which will not contribute significantly during the timescale of the astrophysical event. These are, for example, charged-particle reactions on heavy targets in hydrostatic stellar burning. On the other hand, high temperature can establish reaction equilibria. When both forward and reverse reactions become sufficiently fast to reach equilibrium with abundances set at equilibrium values. The equilibrium abundances of nuclei can be derived by using the relations 9.12 and 9.13 in the network equation 9.1 and assuming $\dot{Y} = 0$. Somewhat depending on the density, for $T > 4-5$ GK all reactions are in a full *nuclear statistical equilibrium* (NSE) and the abundances are given by

$$Y_i = G_i\,(\rho N_\mathrm{A})^{A_i-1}\,\frac{A_i^{3/2}}{2_i^A}\left(\frac{2\pi\hbar^2}{m_\mathrm{u}kT}\right)^{\frac{3}{2}(A_i-1)} e^{\frac{B_i}{kT}} Y_\mathrm{n}^{N_i} Y_\mathrm{p}^{Z_i} \quad , \tag{9.14}$$

$$\sum_i A_i Y_i = 1 \sum_i Z_i Y_i = Y_\mathrm{e} \tag{9.15}$$

with Z_i, N_i, A_i, and B_i being the charge, neutron number, mass number, and the binding energy of the nucleus i, respectively, the atomic mass unit m_u, and the abundances of free neutrons Y_n, free protons Y_p, and free electrons Y_e. Here, it is assumed that reactions via the strong and electromagnetic interactions are in equilibrium while the weak interaction is not. Therefore, Y_e can still be time-dependent and thus also the resulting NSE abundances Y_i.

At $T < 4$ GK and/or low densities only some reactions may be in equilibrium while others are too slow. This gives rise to the so-called *quasi-statistical equilibrium* (QSE) where only groups of nuclei are equilibrated and those groups are connected by slower reactions which are not in equilibrium (Hix et al., 1999). Abundance ratios within a QSE group can be determined by application of Eq. 9.14 while the connecting, slow reaction determines the amount of matter in each group relative to the other groups at a given time. QSE occurs in low temperature, low density Si-burning and in O-burning of stars. Often, the slowest rate falling out of equilibrium first is that of the strongly density-dependent triple-α reaction.

A special case of a QSE is the *waiting-point approximation*, often used in r-process calculations (Cowan et al., 1991; Arnould et al., 2007). There, the network is reduced to neutron capture reactions and their reverse reactions, and β^--decay (with possible release of neutrons). Assuming equilibrated capture and photodisintegration, QSE within an isotopic chain is obtained and the relative abundances are given by

$$\frac{Y_{i+1}}{Y_i} = n_\mathrm{n}\frac{G_{i+1}}{2G_i}\left(\frac{A_i+1}{A_i}\right)^{3/2}\left(\frac{2\pi\hbar^2}{m_\mathrm{u}kT}\right)^{3/2} e^{\frac{Q_\mathrm{ncap}}{kT}} \quad . \tag{9.16}$$

The neutron number density is denoted by n_n and the neutron capture Q-value is given by the neutron separation energy in nucleus $i+1$: $Q_\mathrm{ncap} = S_{\mathrm{n},i+1}$. The indices

i are ordered by increasing neutron number. The β^--decays are much slower and not in equilibrium. Synthesis of the next element is delayed until the decay of the produced isotopes. Typically, only one or two nuclides have significant abundances in such an isotopic QSE chain, hence the name waiting-point approximation.

The advantage of using equilibria is that the rates – and thus the cross sections – do not have to be known explicitly. The resulting abundances are completely determined by basic nuclear properties and the conditions in the astrophysical environment.

9.2 Relevant Energy Range of Astrophysical Cross Sections

In the general calculation of the reaction rate according to Eq. 9.10 the nuclear cross section has to be known. Although the integration limits in Eq. 9.10 run from Zero to Infinity, significant contributions to the integral only come from a comparatively narrow energy range. This is due to the shape of the MB distribution, showing a peak around the energy $E_{\mathrm{MB}} = kT$ and quickly approaching very small values both towards $E = 0$ and $E \gg kT$. For a slowly varying cross section (as found, e.g., in non-resonant neutron-induced reactions), the relevant energy range is simply given by the peak of the distribution, $E_0 = E_{\mathrm{MB}}$ and its width $\Delta_0 = \Delta_{\mathrm{MB}}$. For partial waves higher than s-waves, the additional centrifugal barrier introduces a stronger energy dependence in the cross section and shifts the relevant range to slightly higher energy, i.e. $E_0 \approx 0.172 T_9(\ell + 1/2)$ MeV and $\Delta_0 \approx 0.194 T_9 \sqrt{\ell + 1/2}$ for partial waves $\ell > 0$ (Rauscher et al., 1997; Wagoner et al., 1969). Charged-particle cross sections exhibit a strong energy dependence at energies close to and below the Coulomb barrier. They decrease by many orders of magnitude towards lower energy. Using the astrophysical S-factor

$$S(E) = \sigma E e^{2\pi\eta} \quad , \tag{9.17}$$

with η being the Sommerfeld parameter describing the barrier penetrability, most of the Coulomb suppression is taken out and $S(E)$ is easier to handle because it is varying less with energy than σ. Inserting definition 9.17 into Eq. 9.10 shows that the penetration factor causes a significant shift of the relevant energy range towards higher energy. The resulting energy window (the *Gamow window*, given by the *Gamow peak* appearing when folding the charged particle cross section with the MB distribution) can be approximated by Iliadis (2007); Rauscher et al. (1997)

$$E_0 = 0.12204 \left(Z_1^2 Z_2^2 \mu\right)^{1/3} T_9^{2/3} \quad \mathrm{MeV} \tag{9.18}$$

$$\Delta_0 = 4\sqrt{\frac{E_0 kT}{3}} = 0.23682 \left(Z_1^2 Z_2^2 \mu\right)^{1/6} T_9^{5/6} \quad \mathrm{MeV} \quad . \tag{9.19}$$

Here, T_9 is the plasma temperature in GK. The idea of a single, relevant energy window is only viable for non-resonant cross sections or reactions with broad resonances. Strong, narrow resonances lead to fragmentation of the peak and split it

up in several small energy ranges around the resonance energies, with decreasing weight towards higher energy.

It is important to note that Eq. 9.18 is not always valid. It is based on the assumption that the energy dependence of the cross section is mainly determined by the penetration of the projectile through the Coulomb barrier. However, the dependence is dominated by the one of the smallest width in the entrance or exit channel for resonant reactions or smallest *averaged* width in the case of Hauser-Feshbach compound reactions (see Sec. 9.3.2). This smallest width can also be the one of the exit channel, leading to a different maximum in the contribution to the reaction rate integral than estimated from Eq. 9.18. This is often the case in capture reactions when $\Gamma_{\text{projectile}} \gg \Gamma_\gamma$ (Iliadis, 2007; Newton et al., 2007). Because of the weak energy dependence of the γ-width, there would not be a Gamow window. Effectively, however, the Gamow window is shifted to energies where $\Gamma_{\text{projectile}}$ (which is strongly energy dependent) becomes smaller than Γ_γ. Since reaction rates at higher temperature are determined by cross sections at higher energy, the discrepancy between Eq. 9.18 and the true maximum of the integrand is more pronounced at high temperature than at low temperature. Therefore, the relevant energy range for reactions in explosive burning should be derived by a proper inspection of the product of the (predicted) cross sections and the MB distribution (see Rauscher (2010) for details). For other charged particle captures in astrophysics, often $\Gamma_{\text{projectile}} \ll \Gamma_\gamma$ due to the low interaction energy implied by $E_{\text{MB}} = kT = T_9/11.6045$ MeV, unless for light nuclei (with low Coulomb barrier). Regarding neutron captures, although $\Gamma_{\text{n}} \gg \Gamma_\gamma$ will apply in most cases (unless very close to the reaction threshold), the shape of the integrand is mostly determined by the shape of the MB distribution and obviously not by any Coulomb penetration. Therefore, the relevant energy window for neutrons can still be estimated from the MB distribution as shown above.

9.3 Nuclear Reaction Models

Having determined the relevant energy range, the cross sections have to be predicted by reaction models or determined experimentally. As previously mentioned, often measurements for astrophysics prove difficult due to small cross sections or/and unstable nuclei involved. However, even if a measurement is feasible, the resulting cross section has to be corrected for effects of electron screening and thermal excitation of the target via theoretical models before being used to compute an astrophysical reaction rate.

Here, we provide a brief overview of approaches to predict low-energy cross sections of reactions involving the strong force. Decays and other reactions via the weak force are important but cannot be discussed due to limited space. The reader is referred to other sources, e.g. (Möller et al., 2003; Fuller et al., 1982; Vogel, 2006) and references therein. We also do not cover fission reactions which are important in extremely neutron-rich explosive environments where a r-process could occur and reach the region of fissionable nuclei. Current predictions of fission barriers,

however, carry large uncertainties. For details, see e.g. (Cowan et al., 1991; Arnould et al., 2007; Panov et al., 2005; Goriely et al., 2009; Panov et al., 2010) and references therein. We also only discuss reactions between a nucleus and a nucleon or an α-particle as the majority of reactions in astrophysics is of that type.

The interaction of a particle with a nucleus can excite few or many degrees of freedom, i.e. transfer energy to few (or none) or to many of the nucleons constituting the target nucleus. In nature, all interaction types are, in principle, possible but often only one will be dominating at a given interaction energy but with gradual transitions from one type to the other within certain energy intervals. For theory, it is simpler to consider extreme, idealized cases. Interdependence and interference effects between different reaction mechanisms, even if in principle understood, are very difficult to predict and especially so for the required large number of reactions with unstable nuclei required in astrophysics. In the following we introduce a selection of relevant reaction mechanisms considered in literature. The number of degrees of freedom which can be excited depends on the number of states or levels present in the system formed by projectile and target (Descouvemont et al., 2006). Therefore, it is helpful to distinguish between compound systems with low and high level densities.

9.3.1 Resonance and Potential Models

Low level-density systems exhibit no or only few, isolated resonances in the relevant energy range. These involve mostly light nuclei which have few, widely spaced excited states within several tens of MeV above the ground state and therefore also show only few resonances even when the separation energy of the projectile from the compound system is large. A similar situation also occurs for heavier nuclei with closed shells or heavier nuclei far off stability and close to the driplines where the projectile separation energy becomes very low (e.g. in neutron capture on extremely neutron-rich nuclei) and in consequence the compound system is formed at very low relative energy.

In principle, isolated resonances can be included by the *Breit-Wigner formula* (Blatt, et al., 1991)

$$\sigma^x = \frac{\omega^2}{4\pi}\frac{2J+1}{(2J_x+1)(2J_{\rm proj}+1)}\frac{\Gamma_a^x\Gamma_b}{(E-E_{\rm res})^2+\frac{\Gamma_{\rm tot}^2}{4}} \quad , \tag{9.20}$$

where J and $E_{\rm res}$ refer to the spin and energy of the resonance, ω is the de Broglie wavelength, and $\Gamma_{\rm tot}$ is the total resonance width, including the entrance and exit widths Γ_a^x and Γ_b plus all other open channels. Note that the widths are energy dependent. For a narrow resonance, inserting the above in Eq. 9.10 yields

$$N_{\rm A}\langle\sigma v\rangle = 1.54\times10^{11}\frac{1}{(\mu T_9)^{3/2}}\frac{2J+1}{(2J_x+1)(2J_{\rm proj}+1)}\frac{\Gamma_a^x\Gamma_b}{\Gamma_{\rm tot}}e^{-\frac{11.6045E_{\rm res}}{T_9}} \quad . \tag{9.21}$$

This gives the reactivity in units of $\mathrm{cm^3 s^{-1} mole^{-1}}$ when the widths and the resonance energy E_{res} are inserted in units of MeV (Iliadis, 2007). (Note that the above equations do not involve stellar cross sections. For a true stellar cross section and rate, a thermally weighted sum of target states has to be used, according to Eq. 9.8.) However, tails of resonances with the same J may interfere and there may also be interference with a direct component (see below). Therefore, additional interference terms may have to be added (see, e.g., (Rauscher et al., 1996)). Furthermore, location of the resonance and the widths have to be predicted from nuclear structure. Currently, this is not possible from first principles (except for the lightest nuclei) with the accuracy needed in applications. Therefore, this information usually has to come from experiments.

Instead of Breit-Wigner formulas and interference terms, often the *R-matrix method* (Lane et al., 1958) is used. It is applied to parameterize experimentally known cross sections with as few parameters as possible, implicitly accounting for resonances and their interference. The R-matrix approach can be used to extrapolate the nuclear cross section from existing data to the Gamow range as long as nuclear structure information about resonance levels and non-resonant reaction contributions are included.

In addition to possible resonance contributions a direct capture process can occur. These are fast, one-step processes in which a captured particle directly enters the final state. Typical reaction timescales of direct processes are of the order of 10^{-22} s whereas compound reactions, distributing the energy among a large number of nucleons, take of the order of 10^{-16} s. Direct reactions include transfer processes where a particle exchange takes place between projectile and target nucleus, and capture processes in which the projectile is being fully captured by the target nucleus. These two reaction types can be treated in ab initio models, determining the cross sections from wave functions obtained by solving the Schrödinger equation using effective potentials.

For transfer reactions often the *Distorted Wave Born Approximation* (DWBA) (Satchler, 1983; Glendenning, 2004) is used, utilizing optical potentials to compute the cross sections from the overlap integral of distorted scattering wave functions and the bound state wave function. The DWBA implicitly assumes that elastic scattering is dominant while non-elastic contributions can be treated perturbatively.

On the other hand, capture reactions can be calculated with a simple potential model, which is a first-order approach involving an electromagnetic operator describing the emission of photons due to the dynamics in the movement of electric charges (Descouvemont et al., 2006). In the potential model the differential cross section is proportional to the matrix element defined by the overlap of the final state ϕ_β of the final nucleus and the initial state composed of the target wave function ϕ_α and a (distorted) scattering wave of the projectile χ_α. This can be decomposed into an overlap function S of the target and the final nucleus and a radial integral containing the scattered wave $\chi^x_\alpha(r)$, the bound state wave function of the projectile in the target $\phi_{\mathrm{a+A}}$, and the radial form of the electromagnetic operator $\mathcal{O}_{\mathrm{EM}}$ (Kim et al., 1987)

$$\frac{d\sigma^x}{d\Omega} \propto \left|\left\langle \phi_\beta | \mathscr{O}_{\rm EM} | \chi_\alpha \phi_\alpha^x \right\rangle\right|^2 \propto S\,|\phi_{\rm a+A}(r)\mathscr{O}_{\rm EM}(r)\chi_\alpha^x(r)\,dr|^2 \quad . \tag{9.22}$$

The wave functions $\phi_{\rm a+A}(r)$ and $\chi_\alpha^x(r)$ are obtained by solving the radial Schrödinger equation with appropriate effective potentials.

Both approaches, DWBA and potential model, require a renormalization of the resulting cross section through spectroscopic factors S, describing nuclear structure effects by the overlap of initial and final state of the system. These spectroscopic factors have to be obtained from nuclear structure models or by comparison with experiment (Satchler, 1983; Glendenning, 2004).

Microscopic reaction models are first principle methods, starting from effective nucleon-nucleon interactions and treating all nucleons in a Hamiltonian with exact antisymmetrization of the wave functions. Because of this, no artificial distinction between direct and resonant contributions has to be made. Unfortunately, such reaction models are limited to systems of few nucleons. Although the Quantum Monte Carlo method (Pieper et al., 2001) is promising, it is currently limited to $A \leq 10$ and not applicable to continuum states. Cluster models have been often used for light systems so far (see Descouvemont et al., 2006; Descouvemont, 2003, and references therein). They assume that the nucleons are grouped in clusters and use cluster wave functions defined in the shell model and computed with an adapted effective nucleon-nucleon force. The Resonating Group model (RGM) and the Generator Coordinate Method (CGM) are two equivalent implementations differing in the definition of the relative wave function of the clusters (Descouvemont et al., 2006; Descouvemont, 2003).

9.3.2 Statistical Model

In systems with high level density $\rho(J,\pi,E)$, individual resonances cannot be resolved anymore and an average over the overlapping resonances can be used instead (Fig. 9.1). Further assuming that the relative phases are randomly distributed, interferences will cancel and a simple sum of Breit-Wigner contributions can be replaced by a level-density weighted sum of averaged widths $\langle\Gamma\rangle$ over all spins J and parities π (Descouvemont et al., 2006; Gadioli et al., 1992)

$$\begin{aligned}\sigma^x(E) \propto & \frac{1}{(2J_x+1)(2J_{\rm proj}+1)} \\ & \times \sum_{J,\pi}[(2J+1)\rho(J,\pi,E_{\rm c}) \\ & \times \left\langle \Gamma^x_{\rm pro}(\{J_x,\pi_x\}\rightarrow\{J,\pi\},E)\right\rangle \\ & \frac{\left\langle \Gamma_{\rm b}\left(\sum_{J_{\rm fin},\pi_{\rm fin},E_{\rm fin}}(\{J,\pi\}\rightarrow\{J_{\rm fin},\pi_{\rm fin}\},E_{\rm fin})\right)\right\rangle}{\langle\Gamma_{\rm tot}\rangle}\end{aligned}$$

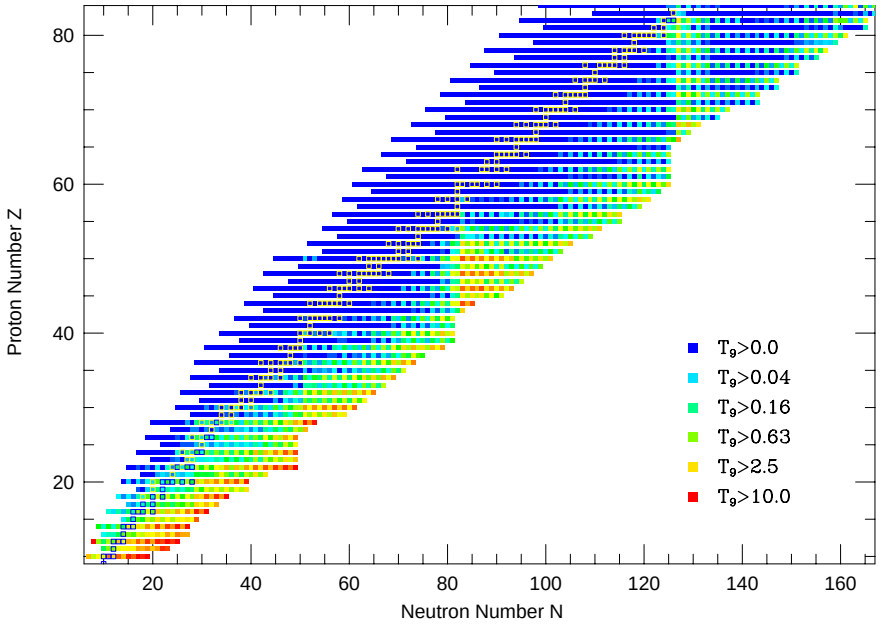

Fig. 9.1 Applicability of the Hauser-Feshbach model to calculate astrophysical reaction rates for neutron-induced reactions: Shown are the stellar temperatures above which the rate can be calculated from Hauser-Feshbach cross sections (reprinted from Rauscher et al., 1997, with permission).

$$\times W(J,\pi,E_{\rm c})] \quad , \tag{9.23}$$

$$E_{\rm c} = E + E_{\rm sep,pro} - E_x \quad , \tag{9.24}$$

$$E_{\rm fin} = E_{\rm c} - E_{\rm sep,fin} - E_{x,\rm fin} \quad . \tag{9.25}$$

This is called the *Hauser-Feshbach* or *statistical model of compound reactions* (Hauser et al., 1952). Width fluctuation corrections W account for non-statistical correlations but are only important close to channel openings (Ericson, 1960). The separation energy $E_{\rm sep,pro}$ of the projectile in the compound system determines at which energy $E_{\rm c}$ the compound system is formed. The averaged width of the exit channel $\langle \Gamma_{\rm b} \rangle$ usually includes a sum over energetically possible final states at energy $E_{x,\rm fin}$ or an integral over a level density of the final system when individual states are not known or numerous. For capture, compound and final system are identical. The averaged widths are related to transmission coefficients $\mathscr{T} = 2\pi\rho\,\langle\Gamma\rangle$. The latter are calculated from the solution of a (radial) Schrödinger equation using an optical potential. (It is to be noted that these potentials differ from the ones employed for low-density systems described in Sec. 9.3.1.)

The challenge for nuclear astrophysics lies in the determination of globally applicable descriptions of low-energy optical potentials as well as level densities, masses (determining the separation energies), and spectroscopy (energies, spins, parities) of low-lying excited states, to be applied for a large number of nuclei at and far

from stability. For details on the different properties and the remaining open problems in their treatment (see, e.g., Descouvemont et al., 2006; Rauscher et al., 1997; Arnould et al., 2007; Goriely et al., 2008; Rauscher, 2011, and references therein). For a general discussion of the applicability of the statistical model, see Rauscher et al. (1997, 2000a); Rauscher (2011).

9.4 Experimental Facilities and Techniques

The experimental determination or verification of nuclear reaction rates requires a large variety of facilities and techniques. This is in particular true if one wants to establish experimentally reaction rates associated with the production of long-lived radioactive isotopes associated with galactic gamma sources. Nuclear astrophysics related experiments include low energy high intensity accelerator measurements with stable beams to study charged particle reactions of relevance for quiescent stellar burning which may possibly lead to the production of ^{7}Be, ^{22}Na and ^{26}Al. High flux neutron beam studies to explore neutron induced reactions for the weak and main s-process which can be associated with the production of long-lived radioactive isotopes such as ^{60}Fe and ^{98}Tc. Real and virtual photon beams are increasingly used for probing nuclear reactions associated with explosive nucleosynthesis events such as the p-process but can also be used to probe indirectly neutron capture reactions associated with the s-process. Intense radioactive beams are the primary tools for exploring nuclear reactions and decay mechanisms far of stability which are expected to occur in explosive stellar environments and may lead to the production of long-lived radioactive elements such as ^{18}F, ^{26}Al, ^{44}Ti and ^{56}Ni.

9.4.1 Low-energy Facilities, Underground Techniques

Low energy charged particle measurements belong to the most challenging experiments in nuclear astrophysics. The cross sections need to be measured at the extremely low energies associated with the Gamow range of quiescent stellar burning. This requires to determine the cross sections of proton capture reactions for hydrogen burning in main sequence stars at energies well below 100 keV. Measurements for helium burning in red giant stars need to be explored in the 200 keV to 500 keV range and heavy ion fusion reactions in subsequent stellar evolution phases need to be measured near 1 MeV to 2 MeV center of mass energy. The cross sections are extremely low, typically in the femto-barn range, which requires a long time, in excess of days, to accumulate a statistical relevant amount of reaction yield data. Typical experimental techniques are summarized in the text book literature (Iliadis, 2007) and will not be discussed here.

The critical issue with low cross sections is that the yield of reaction events is low in the detectors measuring the characteristic gamma or particle radiation produced.

This requires using high efficiency detector material with high resolution to separate the characteristic events from random background events. High beam intensity is desired to increase the event rate, however it may also increase beam induced background on target impurities and is limited by target stability.

The second critical issue is the background rate in the detector. There are typically three different kind of background, cosmic ray induced background in the detector environment, natural long-lived radioactivity in the detector material and the surrounding environment, and beam induced background on low Z target impurities and beam defining slits or apertures. This background must be reduced as far as possible to identify reaction events in the spectrum.

Cosmic ray induced background affects the spectra up to very high energies and makes it difficult to extract weak signals. That background is the most important to remove. Natural environmental background will be strong in an underground environment except for salt mine locations. But the characteristic γ lines are mainly below 3 MeV and can be shielded locally. Neutron background is more difficult to absorb and needs special shielding arrangements. Beam induced background depends critically on the target as well as the choice and preparation of the target material. It is difficult to suppress and may require active shielding procedures.

This can be done by identifying the event electronically by its particular characteristics such as coincidence conditions in a particular decay sequence, pulse shape or timing conditions and reject the background events which do not fulfill these requirements. This can lead to active background suppression by up to three orders of magnitude (Runkle et al., 2005; Couture et al., 2008). While this clearly helps in many cases a more efficient background reduction is desired.

The high energy cosmic ray induced background can be most successfully suppressed by operating the experiments in a deep underground environment where the cosmic ray flux is heavily reduced. This was demonstrated with the installation of the LUNA accelerator facility at the Gran Sasso deep underground laboratory in Italy. The cosmic ray induced background was successfully removed and several critical reactions of the pp-chains and the CNO cycles were successfully measures in the or near the Gamow energy range (Costantini et al., 2009). As a consequence of this successful operation new underground accelerator facilities are being proposed or planned which would allow to cover reactions over a wider energy range than available at LUNA. This is of particular importance for an improved R-matrix analysis and extrapolation. Higher energies are also of great relevance for the underground measurements of α capture reactions and stellar neutron sources in helium burning. In particular it will also improve the chances for pursuing heavy ion fusion reaction studies towards lower energies. There are presently three major initiatives for the construction of new underground accelerator facilities. The proposal to establish an underground accelerator facility ELENA at the Boulby salt mine in the UK seeks to take advantage of the reduced level of neutron and natural activity in a salt environment. The disadvantage will be the reduced depth level compared to the Gran Sasso location. The second proposal is for the development of a two accelerator facility DIANA at the DUSEL underground laboratory at Homestake mine in South Dakota. The third proposal in debate is the construction of an accelerator

Fig. 9.2 The *Dragon* facility in Vancouver, Canada, is an example of nuclear experiment facilities, now aimed at experiments for astrophysically-relevant reactions: Radioactive isotopes can be selected and accelerated to form projectiles for such reactions of interest.

facility in an abandoned train tunnel in the Pyrenees mountains at Canfranc, Spain. With these facilities the community hopes to address the new and critical questions about stellar reaction cross sections and provide the final answer on the nuclear engine of stellar evolution.

However, it has been demonstrated that alternative inverse kinematics methods are a very powerful tool in reducing the background. They are based on the technique of using a high intensity heavy ion beam on a hydrogen or helium gas target and separate the heavy ion recoil reaction products from the primary beam through a high resolution electromagnetic mass separator system from the primary beam. This method has been demonstrated to be successful at a number of different separator facilities such as DRAGON at TRIUMF, Vancouver (Vockenhuber et al., 2007) (Fig. 9.2) and ERNA at the Ruhr University Bochum (Di Leva et al., 2009).

The detection of the recoiling charged particle has a clear efficiency advantage compare to the gamma detection. The possible detection of the gamma rays in coincidence with the reaction products reduces dramatically the backgrounds. However, there are several experimental challenges associated with using recoil separators. At the low stellar energies, the energy spread and the angular aperture are much larger than the acceptance of any of the cited existing recoil separators. In order to measure an absolute cross section the transmission of the recoils should ideally be 100% or

exactly known. It is also necessary to know precisely the charge state distribution of the recoil products. In addition, since the primary beam intensity is typically many orders of magnitude larger than the recoiling reaction products, a large spatial separation between the reaction products and the beam is required, which is difficult to realize for beams with a large energy spread. Therefore, solar fusion reactions are particularly challenging to measure with recoil separators and are typically used for higher energies and for the helium or heavy ion burning reactions.

Dedicated next generation separators for low energy nuclear astrophysics studies with stable ion beams coming on line are the ST.GEORGE facility in Notre Dame (Couder et al., 2008) and the modified and upgraded ERNA facility at CIRCE in Caserta, Italy. Both separators feature large angular and energy acceptance and will be equipped with high density gas jet targets, which will ensure a well defined interaction region.

9.4.2 Laboratory Neutron Sources

Many of the observed or anticipated long lived radioactive isotopes in our galaxy are produced by neutron induced nucleosynthesis in the weak or main s-process taking place in helium and carbon burning stellar environments. This includes ^{41}Ca, ^{60}Fe, ^{63}Ni, but also more massive isotopes such as ^{98}Tc and ^{99}Tc and possibly numerous long lived isomers.

The study of neutron induced stellar reactions leading to the production of such isotopes requires high intensity neutron sources with a well defined energy distribution to determine the reaction cross sections at stellar energies of a few keV. Neutrons in that energy range can be produced in several ways. Nuclear reactions such as ^{7}Li(p,n) or ^{3}H(p,n) with high intensity proton beams provided by low-energy particle accelerators offer the possibility of tailoring the neutron spectrum to the energy range of interest; this has the advantage of low backgrounds. A particularly successful approach is to simulate a quasi-stellar neutron spectra in the laboratory. In bombarding thick metallic lithium targets with protons of 1912 keV, the resulting neutrons exhibit a continuous energy distribution with a high-energy cutoff at E_n = 106 keV and a maximum emission angle of 60 degrees. The angle-integrated spectrum corresponds closely to a Maxwell-Boltzmann distribution for kT = 25 keV (Ratynski et al., 1988). Hence, the reaction rate measured in such a spectrum yields immediately the proper stellar cross section.

Higher intensities can be achieved via photon production by bombarding heavy-metal targets with typically 50-MeV electron beams from linear accelerators. When these energetic neutrons are slowed down in a moderator, the resulting spectrum contains all energies from thermal energy to nearly the initial energy of the electron beam. Since the astrophysical relevant range corresponds to only a narrow window in this spectrum, background conditions are more complicated and measurements need to be carried out at larger neutron flight paths. In turn, the longer flight paths are advantageous for neutron-resonance spectroscopy with high resolution.

The most intense keV neutron flux is produced by spallation reactions. The LANSCE facility at Los Alamos is particularly suited for neutron TOF work due to the favorable repetition rate of only 12 Hz (Lisowski et al., 1990), and because the accumulation of a number of beam pulses in an external storage ring yields extremely intense neutron bursts. Accordingly, excellent signal-to-background ratios can be achieved. The n_ToF facility at CERN provides high intensity neutron beam pulses with a lower repetition rate of 0.4 Hz (Borcea et al., 2003). This has proved highly advantageous for a large number of experimental neutron capture studies along the s-process path.

The experimental methods for measuring (n,γ) cross sections fall into two groups: TOF techniques based on the detection of the prompt capture γ rays and activation methods.

The TOF techniques can be applied in measurements of most stable nuclei but require a pulsed neutron source to determine the neutron energy via the flight time between target and detector. Capture events in the samples are identified by the prompt γ ray cascade in the product nucleus.

The best signature for the identification of neutron capture events is the total energy of the capture gamma cascade, which corresponds to the binding energy of the captured neutron. Hence, accurate measurements of (n,γ) cross sections require a detector that operates as a calorimeter with good energy resolution and is insensitive to neutron exposure. In the gamma spectrum of such a detector, all capture events would fall in a line at the neutron binding energy (typically between 5 and 10 MeV), well separated from the gamma-ray backgrounds that are inevitable in neutron experiments. Such detectors have been successfully developed at the various laboratories using arrays of 4π BaF_2 scintillator detectors with a large number of independent detector modules (Heil et al., 2001) and have emerged as standard technology for these kinds of measurements.

A completely different approach to determining stellar (n,γ) rates is activation in a quasi-stellar neutron spectrum. Compared with the detection of prompt capture gamma rays, this method offers superior sensitivity, which means that much smaller samples can be investigated. Since it is also selective with respect to various reaction products, samples of natural composition can be studied instead of the expensive enriched samples required by the TOF techniques. However, the activation technique is restricted to cases where neutron capture produces an unstable nucleus, and it yields the stellar rate only for two thermal energies at kT = 25 and 52 keV. This method is however particulary powerful in obtaining cross sections for reactions producing long-lived radioactive materials which can be identified by their particular decay characteristics and signature. This activation technique has been used for a variety of measurements. The technique can be applied to short-lived products with half-lives in the millisecond range and allows for cross section measurements with uncertainties of a few percent.

9.4.3 Accelerator Mass Spectroscopy

Classical activation techniques require a characteristic decay signal associated with the decay pattern or the half-life of the produced radioactive isotope. This can be difficult in cases where no characteristic gamma or particle decay pattern exists or where the decay analysis of the β decay signal is prohibited by high background activity. In these cases activation analysis through accelerator mass spectrometry (AMS) offers a powerful tool to measure cross sections through ultra-low isotope-ratio determination. The AMS method was successfully introduced for the study of the neutron-capture cross section of ^{62}Ni(n,γ)^{63}Ni (Nassar et al., 2005), and extended to other neutron and charge-particle-induced reactions, such as ^{25}Mg(p,γ)^{26}Al (Arazi et al., 2006) and ^{40}Ca(α,γ)^{44}Ti (Nassar et al., 2006).

In these cases samples were either irradiated in a neutron spectrum resembling a stellar Maxwell Boltzmann distribution or by charged particles of well known energies. After the irradiation the samples must be chemically treated to extract the radioactive reaction products. This requires some time and limits AMS activation studies to more longer lived isotopes. Since isotopic and isobaric interferences may represent a major challenge in AMS measurements of irradiated samples, extensive background studies for these isotopes are always necessary prior to the irradiations in order to demonstrate that the required sensitivity can be reached. In AMS, negative ions are extracted from an ion source which have to pass a low energy mass spectrometer prior to entering a tandem accelerator. When passing the stripper, positive ions are produced while within this stripping process molecular isobars are destroyed. One positive charge state is selected with a second (high-energy) mass spectrometer system which is optimized for mass, charge and isobar separation trough possible combination of dipole magnet separators, Wien-filters, and more recently magnetic gas filled separators for improved isobar separation. With such a system the concentration ratio of the radioisotope is determined relative to a stable isotope by measuring the number of radionuclides relative to the current of the isotopic ions in front of the detector, after adjusting the injector magnet, terminal and Wien-filter voltage appropriately. By measuring relative to a standard sample of known isotopic ratio, factors like stripping yields and transmissions mostly cancel.

The difficulties with AMS experiments is in the chemical preparation of the sample and the sufficient separation of the extracted radioactive ions from background events. While AMS is a widely established method with many applications, the analysis of the very limited number of radioactive products from low cross section reactions remains challenging. Systematic studies are necessary to reduce possible uncertainties.

Dedicated AMS facilities with an established nuclear astrophysics program are the Vienna Environmental Research Accelerator (VERA) (Kutschera et al., 1997), the Center for Isotopic Research on Cultural and Environmental Heritage (CIRCE) in Caserta/Italy (Terrasi et al., 2007) or the Munich Tandem accelerator facility (Knie et al., 2000) which is optimized for the analysis of more massive radioactive isotopes. A new AMS program is presently being developed utilizing the Notre Dame tandem accelerator (Robertson et al., 2007).

9.4.4 Radioactive Beam Techniques

The development of radioactive accelerated beams for low energy nuclear astrophysics experiments has been one of the large challenges of the field. The experimental study of nuclear reactions and decay processes far of stability is necessary for the understanding of explosive nucleosynthesis processes such as the rp-process in cataclysmic binary systems or the r-process and p-process in the supernova shock front. These processes can in particular contribute to the production of long-lived galactic radioactivity by primary reaction or also by secondary decay processes from the reaction path towards the line of stability.

For the purpose of studying the origin of long-lived radioactive isotopes in astrophysical environments radioactive beams are utilized in two ways, for producing long-lived targets by implantation for subsequent irradiation with neutron, charged particle or possibly intense photon beams or for direct reaction measurement in inverse kinematics on light ion target materials. The later approach requires well defined mono-energetic and intense radioactive beams and a detection system for light or heavy recoil reaction products.

The main challenge in this approach is to produce a sufficiently high intensity of radioactive beams which have to be produced on-line as a secondary reaction product. This requires high cross sections for the production process and high primary beam intensities. A variety of different approaches has been chosen in the past to optimize the production efficiency and maximize the intensity of the radioactive beams. A technique developed for small scale facilities is the selection of specific nuclear reactions tailored for the on-line production of radioactive beams at optimum conditions. The secondary particles can be used for subsequent nuclear reaction studies after blocking and separation from the primary beams (Kolata et al., 1989). The efficient separation of a suitably high intensity beam of radioactive species is the most challenging problem for this approach.

An alternative approach is the ISOL (Isotope Separation On-Line) technique where high energy protons are used to bombard heavy ion targets for producing a large number of radioactive species through spallation processes. These isotopes diffuse out of the target into an ion source for being charged and re-accelerated for secondary beam decay or reaction experiments. The method has been proven to be very powerful over the years but is limited to isotopes with lifetimes appreciably longer that the time necessary for the diffusion transport and ionization process. This can be different for different elements because of the associated chemical processes between the isotopes and the surrounding environment.

The third approach is based on the use of energetic heavy projectiles bombarding light or target nuclei fragmenting on impact. This fragmentation process generates a cocktail beam of many radioactive species which move forward with high velocity because the initial momentum of the primary particles is maintained. For experiments with a specific secondary particle, it must be selected by fragment separator systems which separate and focus the isotopes by magnetic fields and energy loss characteristics in heavy wedge materials. For nuclear astrophysics related experiments the fast beam particles need to be slowed down by energy loss in gas or solid

material and re-accelerated to energies corresponding to the temperatures in the explosive stellar scenarios.

There is a number of laboratories which have focused on nuclear reaction studies with radioactive beams. The first fully operating radioactive beam laboratory based on the ISOL principle was the coupled cyclotron facility at Louvain la Neuve which did a number of successful radioactive beam studies of relevance for investigating the the production of ^{18}F in novae (De Sérville et al., 2009). These measurements were complemented by measurements at the HRIBF facility at Oak Ridge using intense ^{18}F beams (Chae et al., 2006). Both facilities produce the radioactive species by nuclear reactions on thin production targets, with the reaction products being transported into an ion source for producing and subsequently accelerating the secondary beam. The intensity is largely limited by target technology and beam transport and re-ionization efficiency.

The premier ISOL radioactive beam facility is ISAC at TRIUMF Canada. The primary 600 MeV proton beam is provided by the TRIUMF cyclotron. The reaction products are post-accelerated in an RFQ SC LINAC accelerator combination to energies of 0.3 to 3 MeV/u. ISAC has successfully performed a number of radioactive beam experiments of relevance for explosive hydrogen and helium burning. Most notable a direct study of ^{21}Na(p,γ)^{22}Mg in inverse kinematics to probe the production mechanism of ^{22}Na in Ne nova explosion environments (D'Auria et al., 2004). The facility also runs a successful program with stable beams which was utilized to investigate the production of ^{44}Ti (Vockenhuber et al., 2007). Presently a number of studies associated with the production of the long-lived γ emitter ^{26}Al are being performed.

Other ISOL based radioactive beam facilities such as Spiral facility at GANIL in Caen, France or REX-ISOLDE at CERN have been used to perform interesting experiments for nuclear astrophysics but have been less concerned with the question of nuclear production mechanisms for long lived cosmic gamma emitters.

There have been a number of fast radioactive beam facilities with scientific programs in nuclear astrophysics primarily aimed at the study of nucleosynthesis processes far off stability. However the rapid new developments in fast beam physics promises a number of new experimental opportunities which can provide benefits for studying reactions associated with the production of long-lived gamma emitters in explosive nucleosynthesis events.

There are currently four major fragmentation facilities in the world: GANIL and GSI in Europe, NSCL/MSU in the US and RIKEN in Japan. They are all based on Heavy Ion accelerators which operate in complementary energy domains. Because of the high energy of the fragment products low energy reaction experiments for nuclear astrophysics are not possible but the development of indirect techniques to determine critical reaction or decay parameters has been the primary goal. In the context of long-lived isotopes of astrophysical interest a major contribution was the development of fast beams such as ^{8}B at NSCL/MSU, RIKEN, and GSI for utilizing Coulomb dissociation techniques for probing critical reactions such as ^{7}Be(p,γ)^{8}B. The NSCL and RIKEN also successfully developed a ^{44}Ti beam for new measurements of its half-life (Görres et al., 1998). More half-life measurements of long-lived

isotopes such as ^{60}Fe are presently underway to re-evaluate these critical parameters.

9.5 Specific Experiments

The complexities of the experiments and the uncertainties in the experimental results affect the reliability of model predictions on the nucleosynthesis of long-lived radioactive species. In particular recent studies of critical nuclear reactions and decay processes exhibit considerable differences to earlier studies which so far have been the reference point for nucleosynthesis simulations and predictions for long-lived radioactive isotope abundances in stellar burning environments. It is therefore important to carefully evaluate the experimental results and clarify possible discrepancies and inconsistencies in the data. This section will discuss the present status of the experimental reaction rates and evaluate future opportunities to improve the existing data base.

9.5.1 Experiments with Stable Beams

Many of the long-lived radioactive gamma emitters in our universe have been produced by radiative capture reactions on stable isotopes. The best known examples are ^{26}Al, which is primarily formed by proton capture on stable ^{25}Mg isotopes, ^{25}Mg(p,γ)^{26}Al, and ^{44}Ti which is most likely produced via alpha capture on stable ^{40}Ca isotopes, ^{40}Ca(α,γ)^{44}Ti. Extensive measurements using in-beam γ spectroscopy techniques have been made for both reactions and have formed the basis for earlier reaction rate compilations.

The low energy reaction cross section of ^{25}Mg(p,γ)^{26}Al is characterized by several resonances with energies between 30 keV and 400 keV . The reaction rate is directly correlated to the strengths $\omega\gamma$ of the resonances. The strengths for the resonances above 190 keV have been determined from the on-resonance thick target yield in radiative capture measurements (Elix et al., 1979; Iliadis et al., 1990). The strengths of lower energy resonances are estimated on the basis of single particle transfer reaction studies. Of particular importance are three resonances at 90 keV, 130 keV and at 190 keV which determine the reaction rate at temperatures typical for stellar hydrogen burning in AGB stars and nova explosions. Because the low energy radiative capture measurements have been handicapped by cosmic ray induced background, an alternative measurement was done using the AMS technique to analyze the number of ^{26}Al reaction products after irradiation at resonance energies (Arazi et al., 2006). The experiment was successful and confirmed the resonance strengths of the known resonances at 304 keV, 347 keV, and 418 keV resonance energy. However the results indicated a substantially lower strength for the critical resonance at 190 keV. This would reduce the reaction rate by about a factor of five at

the temperature range between 0.2 and 1.0 GK. This result introduced a large uncertainty in the reaction rate which motivated a new experimental study at LUNA in the Gran Sasso laboratory using in-beam gamma spectroscopy techniques with a variety of high efficiency and high resolution gamma detector devices. The measurements confirmed earlier gamma spectroscopy studies of the strengths of higher energy resonances (Elix et al., 1979; Iliadis et al., 1990) tabulated in the NACRE compilation (Angulo et al., 1999). The new results are being prepared for publication. Parallel to the gamma spectroscopy measurement, the irradiated samples were analyzed for their ^{26}Al content using AMS techniques. The AMS measurements were performed at the CIRCE facilities. Excellent agreement is demonstrated for the resonance at 304 keV, additional experiments are being pursued for lower energy resonances to address the inconsistencies in the strength determination for the 190 keV resonance.

The ^{40}Ca$(\alpha,\gamma)^{44}$Ti reaction is considered to be one of the major production reactions for ^{44}Ti in supernova shock front nucleosynthesis. The cross section for this radiative capture process has been explored in a number of in-beam gamma spectroscopy studies down to center of mass energies of 2.5 MeV (Simpson et al., 1971; Cooperman et al., 1977). The cross section is characterized by a large number of resonances and the initial reaction rate determinations were based on an analysis of resonance strengths. Despite the high level density in ^{44}Ti, it was noted that the experimental reaction rate is substantially smaller than the reaction rate based on statistical model Hauser Feshbach predictions (Rauscher et al., 2000b). The reaction was studied independently using a thick He-gas cell target and counting the long lived ^{44}Ti reaction products by AMS techniques (Nassar et al., 2005) to determine the integral yield over an energy range of 1.7 to 4.2 MeV. The extracted reaction rate is substantially higher than the ones discussed in the literature (Rauscher et al., 2000b). A more recent study of the reaction using inverse kinematics techniques was performed at the ISAC facility at TRIUMF, Vancouver, separating the ^{44}Ti reaction products on-line with the DRAGON recoil separator. The measurements covered the energy range of 2.3 MeV to 4.2 MeV (center of mass) in more than 100 small energy steps. The extracted yield was mostly interpreted as on-resonance resonance thick target yield and translated to a resonance strength. There are large uncertainties associated with this approach, in particular with the determination of the resonance energies, which have not been unequivocally determined in the experiment. In some cases several of the quoted resonances agree with previously identified states, in other cases it needs to be confirmed that the observed yields really correspond to additional resonances and do not originate from tail contributions of resonant yield curves associated with the different states. As far as the resonance levels which have been observed in both studies are concerned the published strengths are comparable to each other. Nevertheless the reaction rate suggested by Vockenhuber et al. (Vockenhuber et al., 2007) is larger by more than a factor of two than the rates projected on the basis of the in-beam gamma spectroscopy measurements, but it is in agreement with the projections by Rauscher et al. (Rauscher et al., 2000b). The difference is mainly due to the difference in resonance numbers. While the resonance identification in previous work was based on a careful analysis of the particular gamma decay characteristics of the observed levels, the analysis of the recoil data is

insufficient in providing information to differentiate between different resonances. It cannot be excluded that the number of identified states are overestimated; a more detailed gamma spectroscopy study with thin targets is therefore highly advisable to remove the existing uncertainties.

9.5.2 Experiments with Neutron Beams

A particularly interesting case is the origin of the long-lived gamma emitter ^{60}Fe. Its characteristic γ-radioactivity has been observed with the INTEGRAL gamma ray telescope in supernova remnants near the solar system. These observations are complemented by recent AMS studies which suggest high ^{60}Fe abundance in deep sea ferromanganese sediments (Knie et al., 2004). These ^{60}Fe observations have been interpreted as indication for the existence of a recent ($\approx$ 3 million years) supernova event in the solar system vicinity. A more quantitative interpretation of the time and distance of the proposed supernova event requires a detailed knowledge of the nucleosynthesis history of ^{60}Fe.

The radioactive ^{60}Fe isotope is produced by a sequence of neutron capture reactions of stable iron isotopes such as ^{58}Fe(n,γ)^{59}Fe(n,γ)^{60}Fe, the production rate and final abundance of the long-lived ^{60}Fe depends on the reaction rate of these feeding processes as well as on the rate of the ^{60}Fe(n,γ)^{61} depletion reaction. No experimental information are available about the associated cross sections except for the neutron capture reaction ^{58}Fe(n,γ)^{59}Fe. Present simulations of the ^{60}Fe nucleosynthesis rely entirely of statistical model predictions of the neutron capture rates. Because of the relatively low level density in the associated ^{60}Fe, ^{61}Fe compound nuclei these model predictions are unreliable and need to be tested experimentally. This is underlined by the direct comparison between the experimental cross sections for neutron capture on the stable isotopes ^{56}Fe, ^{57}Fe, and ^{58}Fe which were all measured through neutron activation techniques and theoretical Hauser Feshbach predictions which show considerable discrepancies in particular in the cases of ^{56}Fe(n,γ)^{57}Fe and ^{57}Fe(n,γ)^{58}Fe. For ^{58}Fe(n,γ)^{59}Fe on the other hand , the agreement seems reasonable well but that cannot be extrapolated towards neutron captures on the more neutron rich Fe isotopes which are subject of the here proposed measurements.

Particularly important is the determination of the reaction rate of ^{59}Fe(n,γ)^{60}Fe since it competes directly with the ^{59}Fe β-decay which would by-pass the production of ^{60}Fe. A direct measurement of this critical reaction in the traditional activation or time of flight spectroscopy technique is not feasible because the target is radioactive and only small amounts can be accumulated. these small amounts nevertheless produce a large background activity level, which would prohibit any of the described methods. The cross section for the ground state decay branch of ^{59}Fe(n,γ_0)^{60}Fe can however be investigated using inverse ^{60}Fe(γ,n)^{59}Fe Coulomb dissociation techniques. The ^{60}Fe beam can be produced by fragmentation of a heavy ion such as ^{64}Ni on a light Be target at an energy of 500 MeV/u. The ^{59}Fe recoil products, and the released reaction neutrons, as well as γ rays can be detected

with reasonable 200 keV resolution using a combination of a magnetic separator system and a neutron detector wall. This allows particle identification of all reaction products.

9.5.3 Experiments with Radioactive Beams or Targets

The depletion processes of long-lived radioactive isotopes includes the natural decay. Simulating this branch requires not only a good knowledge of the laboratory lifetime but also of the nature of the decay process since extreme environmental effects can change the decay rates drastically. In terms of β decay, the decay can be accelerated through the decay of thermally excited states as in the case of ^{26}Al. For decay through electron capture, the decay can be slowed down since the nuclei are completely ionized and the electrons have to be captured from the stellar plasma rather than from the inner K- or L-shell of the atom. This affects in particular the lifetime of ^{44}Ti, which primarily decays by electron capture.

Often the depletion is primarily driven by nuclear reactions, such as ^{22}Na(p,γ)^{23}Mg, ^{26}Al(p,γ)^{27}Si, ^{44}Ti(α,p)^{47}V, or ^{60}Fe(n,γ)^{61}Fe, but also capture reactions on shorter-lived excited configurations of these nuclei are possible, such as ^{26}Al*(p,γ)^{27}Si. There are two possibilities for experimental studies of the reaction cross sections. The first one is based on the production of highly enriched long-lived radioactive targets, which can be prepared through standard chemical target preparation techniques using externally bred radioactive material, or by implantation of radioactive ions at low energy ISOL facilities. The disadvantage of both techniques is that the actual γ measurements have to be performed in a high radiation background environment produced by the sample itself.

Nevertheless, earlier measurements of reactions such as ^{22}Na(p,γ)^{23}Mg (Seuthe et al., 1990) and ^{26}Al(p,γ)^{27}Si (Buchmann et al., 1984) relied entirely on this approach. In both cases a large number of resonances were detected and the resonance strength determined for calculating the reaction rates. The results for ^{22}Na(p,γ)^{23}Mg were confirmed by new direct measurements using improved target and detection techniques (Stegmüller et al., 1996), resulting in the observation of an additional low energy resonance at lower energies. Complementary spectroscopy techniques such as the study of the β-delayed proton decay of ^{23}Al (Peräjärvi et al., 2000) and the heavy ion reaction induced γ decay of proton unbound states in ^{23}Mg (Jenkins et al., 2004) provided additional nuclear structure information which led to the reduction of uncertainties in the reaction rate.

The situation is similar with ^{26}Al(p,γ)^{27}Si; after the initial study with radioactive targets (Buchmann et al., 1984). A number of transfer experiments (Schmalbrock et al., 1986; Vogelaar et al., 1996) providing complementary information about the threshold levels in ^{27}Si not accessible to direct study by radiative capture measurements lead to an improved reaction rate for ^{26}Al ground state capture. A first direct study of a lower energy resonance was successfully performed in inverse kinematics at the ISAC facility at TRIUMF using the DRAGON recoil sepa-

rator (Ruiz et al., 2006). The resonance value is substantially smaller than the value quoted before (Vogelaar et al., 1996), which reduced the reaction rate slightly at temperatures anticipated for nova burning conditions.

Not included in the reaction rate calculations are possible contributions of proton capture on the thermally first excited state in ^{26}Al (Runkle et al., 2001). Recently number of indirect measurements have been performed to explore the possible contribution to the total reaction rate of ^{26}Al(p,γ)^{27}Si. Transfer reactions have been used to populate proton unbound states in ^{27}Si measuring the subsequent proton decay to the ground state and the first excited state in ^{26}Al (Deibel et al., 2009). This approach allows to determine the branching and the relative strength of the proton decays for each of the unbound states. This can be used to scale the reaction rate component for the proton capture on the first excited state.

Possible lower energy resonance contributions to the proton capture rates on the ground state (Lotay et al., 2009) and the excited state of ^{26}Al (Lotay et al., 2009) have been explored by γ spectroscopy techniques probing the proton unbound state in ^{27}Si through heavy ion fusion evaporation reactions and measuring the γ decay of proton unbound states. This is a particular efficient method to explore the levels near the threshold where proton decay is suppressed by the Coulomb barrier. The measurements provide critical information about spin and parity of the observed states but gives only limited information about the resonance strengths which is primarily determined by the proton decay strength.

The main reaction for the depletion of ^{60}Fe in neutron rich environments is ^{60}Fe(n,γ)^{61}Fe. The reaction rate used for nucleosynthesis simulations was for many years based on theoretical Hauser Feshbach model predictions. Recently an experiment has been performed at the FZK Karlsruhe in Germany to determine the stellar reaction cross section experimentally by neutron activation with the neutron beam resembling a quasi-stellar neutron spectrum (Uberseder et al., 2009). The activated ^{60}Fe sample was prepared from PSI beamstop material. The cross section was determined from the characteristic ^{61}Fe γ activity relative to the amount of ^{60}Fe nuclei in the target material. The latter was determined from the characteristic ^{60}Fe γ activity of the target sample. based on this the experimental results suggest a cross section which is twice as large as standard Hauser Feshbach predictions suggesting a much more rapid depletion of ^{60}Fe in neutron rich environment than previously anticipated. The estimate of the number of ^{60}Fe nuclei, however relied on adopting a half-life of $T_{1/2}$=1.49 Gy (Kutschera et al., 1984). Recent work suggested that the half-live is considerably larger model $T_{1/2}$=2.62 Gy (Rugel et al., 2009). This would translate into a considerably larger amount of ^{60}Fe particles in the sample, suggesting a cross section which would be in fair agreement with the Hauser Feshbach predictions. New independent life time measurements for ^{60}Fe are clearly necessary to address this issue and remove the uncertainty in the interpretation of the radiative capture data.

References

C. Angulo, M. Arnould, M. Rayet, et al. Nucl. Phys. **A656** 3 (1999)
A. Arazi, T. Faestermann, J. O. Fernandez Niello, et al., Phys. Rev. C **74** 025802 (2006)
M. Arnould, S. Goriely, K. Takahashi, Phys. Rep. **450**, 97 (2007)
J. M. Blatt, V. F. Weisskopf, *Theoretical Nuclear Physics* (Dover, 1991)
C. Borcea, P. Cennini, M. Dahlfors, et al., Nucl. Instr. Meth. A **513** 524 (2003)
L. Buchmann, M. Hilgemeier, A. Krauss, et al., Nucl. Phys. **A415** 93 (1984)
K. Y. Chae, D. W. Bardayan, J. C. Blackmon, et al. Phys. Rev. C **74** 012801 (2006)
E. L. Cooperman, M. H. Shapiro, and H. Winkler, Nucl. Phys. **A284** 163 (1977)
J. Cooperstein, J. Wambach, Nucl. Phys. **A420**, 591 (1984)
H. Costantini, A. Formicola, G. Imbriani, et al., Rep. Prog. Phys **72** 086301 (2009)
M. Couder, G.P.A. Berg, J. Görres, et al., Nucl. Instr. Meth. A **587** 35 (2008)
A. Couture, M. Beard, M. Couder, et al, Phys. Rev. C **77** 015802 (2008)
J. J. Cowan, F.-K. Thielemann, J. W. Truran, Phys. Rep. **208**, 267 (1991)
J. M. D'Auria, R. E. Azuma, S. Bishop, et al., Phys. Rev. C **69** 065803 (2004)
De Sérville N, C Angulo, A. Coc, et al. Phys. Rev. C **79** 015801 (2009)
C. M. Deibel. J. A. Clark, R. Lewis, et al., Phys. Rev. C **80** 035806 (2009)
P. Descouvemont, *Theoretical Models for Nuclear Astrophysics* (Nova Science Publications, 2003)
P. Descouvemont, T. Rauscher, Nucl. Phys. **A777**, 137 (2006)
A. Di Leva, L. Gialanella, R. Kunz, et al., Phys. Rev. Lett. **102** 232502 (2009)
K. Elix, H. W. Becker, L. Buchmann, et al., Z. Phys. A **293** 261 (1979)
T. Ericson, Phys. Rev. Lett. **5**, 430 (1960)
G. M. Fuller, W. A. Fowler, M. J. Newman, Ap. J. **252**, 715 (1982)
J. Görres, J. Meißner, H. Schatz, et al., Phys. Rev. Lett. **80** 2554 (1998)
E. Gadioli, P. E. Hodgson, *Pre-Equilibrium Nuclear Reactions* (Clarendon Press, Oxford 1992)
N. K. Glendenning, *Direct Nuclear Reactions* (World Scientific, 2004)
S. Goriely, S. Hilaire, A. J. Koning, Astron. Astrophys. **487**, 767 (2008)
S. Goriely, S. Hilaire, A. J. Koning, M. Sin, R. Capote, Phys. Rev. C **79**, 024612 (2009)
W. Hauser, H. Feshbach, Phys. Rev. **87**, 366 (1952)
M. Heil, R. Reifarth, M. M. Fowler, et al.,Nucl. Instr. Meth. A **459** 516 (2001)
W. R. Hix, F.-K. Thielemann, Ap. J. **511**, 862 (1999)
J. A. Holmes, S. E. Woosley, W. A. Fowler, B. A. Zimmerman, At. Data Nucl. Data Tables **18**, 305 (1976)
C. Iliadis, *Nuclear Physics of Stars* (Wiley-VCH, 2007)
C. Iliadis, T. Schange, C. Rolfs, et al. Nucl. Phys. **A512** 509 (1990)
D. G. Jenkins, C. J. Lister, R. V. F. Janssens, et al., Phys. Rev. Lett. **92** 031101 (2004)
C. W. Johnson, E. Kolbe, S. E. Koonin, K. Langanke, Ap. J. **392**, 320 (1992)
K. H. Kim, M. H. Park, B. T. Kim, Phys. Rev. C **23**, 363 (1987)
K. Knie, T. Faestermann, G. Korschinek, et al., Nucl. Instr. Meth. B **172** 717 (2000)
K. Knie, G. Korschinek, T. Faestermann, et al., Phys. Rev. Lett. **93** 171103 (2004)
J. J. Kolata, A. Morsad, X. J. Kong, et al., Nucl. Instr. Meth. B **40** 503 (1989)
W. Kutschera, P. Collon, H. Friedmann, et al., Nucl. Instr. Meth. B **123** 47 (1997)
W. Kutschera, P. J. Billquist, D. Frekers, et al., Nucl. Inst. Meth. B **5** 430 (1984)
A. M. Lane, R. G. Thomas, Rev. Mod. Phys. **30**, 257 (1958)
P. W. Lisowski, C. D. Bowman, G. J. Russell, S. A. Wender, Nucl. Sci. Eng. **106** 208(1990)
G. Lotay, P. J. Woods, D. Sewryniak, et al., Phys. Rev. Lett. **102** 162502 (2009)
G. Lotay, P. J. Woods, D. Sewryniak, M. P. Carpenter, R. V. E. Janssens, S. Zhu, Phys. Rev. C **80** 055802 (2009)
P. Möller, B. Pfeiffer, K.-L. Kratz, Phys. Rev. C **67**, 055802 (2003)
H. Nassar, M. Paul, I. Ahmad, et al., Phys. Rev. Lett. **94** 092504 (2005)
H. Nassar, M. Paul, I. Ahmad, et al., Phys. Rev. Lett. **96** 041102 (2006)

J. R. Newton, C. Iliadis, A. E. Champagne, A. Coc, Y. Parpottas, C. Ugalde, Phys. Rev. C **75**, 045801 (2007)
I. V. Panov, E. Kolbe, B. Pfeiffer, T. Rauscher, K.-L. Kratz, F.-K. Thielemann, Nucl. Phys. **A747**, 633 (2005)
I. V. Panov, I. Yu. Korneev, T. Rauscher, G. Martínez-Pinedo, A. Kelić-Heil, N. T. Zinner, F.-K. Thielemann, Astron. Astrophys. **513**, A61 (2010); arXiv:0911.2181
K. Peräjärvi, T. Siiskonen, A. Honkanen, P. Dendooven, et al., Phys. Lett. B **492** 1 (2000)
S. C. Pieper, R. B. Wiringa, Ann. Rev. Nucl. Part. Phys. **51**, 53 (2001)
W. Ratynski, F. Käppeler, Phys. Rev. C **37**, 595 (1988)
T. Rauscher, G. Raimann, Phys. Rev. C **53**, 2496 (1996)
T. Rauscher, F.-K. Thielemann, K.-L. Kratz, Phys. Rev. C **56**, 1613 (1997)
T. Rauscher, F.-K. Thielemann, At. Data Nucl. Data Tables **75**, 1 (2000a)
T. Rauscher, F. K. Thielemann, J. Görres, M. Wiescher, Nucl. Phys. **A675** 695 (2000b)
T. Rauscher, A. Heger, R. D. Hoffman, S. E. Woosley, Ap. J. **576**, 323 (2002)
T. Rauscher, Phys. Rev. C **81**, 045807 (2010)
T. Rauscher, Int. J. Mod. Phys. E, in press (2011); arXiv:1010.4283
D. Robertson, C. Schmitt, Ph. Collon, et al., Nucl. Instr. Meth. B **259** 669 (2007)
G. Rugel, T. Faestermann, K. Knie, et al., Phys. Rev. Lett. **103** 072502 (2009)
C. Ruiz, A. Parikh, J. José, L. Buchmann, Jet al., Phys. Rev. Lett. **96** 252501 (2006)
R. C. Runkle, A. E. Champagne, C. Angulo, et al. Phys. Rev. Lett. **94:** 082503 (2005)
R. C. Runkle, A. E. Champagne, J. Engel, Ap J **556**, 970 (2001)
E. E. Salpeter, H. M. Van Horn, Ap. J. **155**, 183 (1969)
G. R. Satchler, *Direct Nuclear Reactions* (Clarendon, Oxford 1983)
P. Schmalbrock, T. R. Donoghue, M. Wiescher, V. Wijekumar, C. P. Browne, A. A. Rollefson, C. Rolfs, A. Vlieks, Nucl. Phys. **A457**, 182 (1986)
S. Seuthe, C. Rolfs, U. Schröder, et al., Nucl. Phys. **A514** 471 (1990)
J. J. Simpson, W. R. Dixon, and R. S. Storey, Phys. Rev. C **4** 443 (1971)
F. Stegmüller, C. Rolfs, S. Schmidt, et al., Nucl. Phys. **A601** 168 (1996)
F. Terrasi, D. Rogalla, N. De Cesare, et al., Nucl. Instr. Meth. B **259** 14 (2007)
E. Uberseder, R. Reifarth, D. Schumann, et al., Phys. Rev. Lett. **102** 151101 (2009)
C. Vockenhuber, C. O. Ouellet, L.-S. The, et al., Phys. Rev. C **76** 035801 (2007)
P. Vogel, Nucl. Phys. **A777**, 340 (2006)
B. Vogelaar, L. W. Mitchell. R. W. Kavanagh, et al., Phys. Rev. C **53** 1945 (1996)
R. V. Wagoner, Ap. J. Suppl. **18**, 247 (1969)
R. A. Ward, W. A. Fowler, Ap. J. **238**, 266 (1980)
D. G. Yakovlev, L. R. Gasques, A. V. Afanasjev, et al., Phys. Rev. C **74**, 035803 (2006)